Evaluation of a regional atmospheric model for January 1993, using in situ measurements from the Antarctic

Nicole P. M. van Lipzig,[1, 2] Erik van Meijgaard,[1] Johannes Oerlemans[2]

[1]*Royal Netherlands Meteorological Institute (KNMI), P.O. Box 201, 3730 AE de Bilt, The Netherlands*
[2]*Institute for Marine and Atmospheric Research Utrecht (IMAU), P.O. Box 80.005, 3508 TA Utrecht, The Netherlands*

ABSTRACT. The performance of a regional atmospheric climate model (RACMO) with a horizontal resolution of 55 km × 55 km is evaluated using measured temperature and humidity profiles. Parameterisations of the physical processes are taken from the EC-HAM4 general circulation model (GCM). Sea-surface temperatures and sea-ice mask in the model are prescribed from observations. The model is forced by re-analyses of the European Centre for Medium-range Weather Forecasts (ECMWF) at the lateral boundaries.

We compared simulations for January 1993 with boundary-layer profiles measured at the Swedish research station Svea (Dronning Maud Land, Antarctica) and with radio-sonde measurements made at the Georg von Neumayer (GvN) and South Polar stations for the same period. This comparison was performed in order to study some model characteristics before the model is used for mass-balance calculations. The vertical temperature gradient at Svea during the night is overestimated by RACMO, but corresponds much more closely to the observations than do the ECMWF re-analyses. In the re-analyses a decoupling of the lowest model layer from the higher atmosphere occurs. The differences between the absolute temperatures at the GvN and SP stations and the absolute temperatures at the model gridpoints corresponding most closely to these sites are less than 5°C. The humidity profiles indicate that the model generally underestimates the turbulent transport of moisture from the surface to higher levels.

1. INTRODUCTION

The mass balance of the Antarctic ice sheet is important for global sea level. Estimates of the surface mass balance, obtained by different methods (e.g. monitoring stakes and dating layers in ice cores or ice pits), have been used to compose climatologies (Giovinetto and Bentley, 1985). However, measuring sites are not spread equally over the continent, and spatial coverage in some areas is small. Since the surface mass balance is determined mainly by the atmospheric circulation, atmospheric models can be used to obtain additional information about this quantity. General circulation models (GCMs) have been used frequently for mass-balance simulations (e.g. Bromwich and others, 1995; Connolley and King, 1996; Marsiat, 1996). Although much progress has been made in recent years, GCMs still reveal many deficiencies with regard to polar regions (Connolley and Cattle, 1994; Genthon, 1994; Tzeng and others, 1994). Atmospheric models have been used for obtaining information on the sensitivity of the surface mass balance to changes in atmospheric conditions. An example of a sensitivity study with a GCM is the one performed by Ohmura and others (1996). Their results confirm the idea that a doubling of atmospheric CO_2 is likely to cause an increase in the mass of the Antarctic ice sheet due to increased poleward moisture transport.

The topography plays an important role in establishing meteorological conditions in the Antarctic. For instance, strong, persistent katabatic winds in the coastal regions constitute an outflow of cold, dry air. Furthermore, orographic lifting of moist air by the ice sheet causes high precipitation rates on the steep coastal slopes of the continent (Bromwich, 1988). These processes can only be simulated satisfactorily when the topography is resolved with sufficient detail. For this, limited-area models (LAMs) or GCMs with a stretched grid can be used, because they provide high resolution and require only limited computing resources compared with models covering the entire globe with the same high resolution. Simulations over Antarctica with LAMs nested in European Centre for Medium-range Weather Forecasts (ECMWF) analyses have been performed with various objectives. Hines and others (1995) employed a cloud-free version of the National Centre for Atmospheric Research mesoscale model version 4 (NCAR MM4) to test the ability of the model to simulate cyclones, katabatic wind and synoptic-scale features in winter. Walsh and McGregor (1996) performed July simulations with the Division of Atmospheric Research limited-area model (DARLAM) and identified some substantial differences between model output and ECMWF analyses. They found that the model represents accumulation well compared to the analysis of Budd and others (1995), although it slightly overestimates accumulation in regions of steep orography and in parts of the interior. Engels and Heinemann (1996) used a simulation with a 25 km² model nested in a 50 km² LAM to study mesocyclones in the Weddell Sea.

The regional atmospheric climate model (RACMO) has been applied recently to several regions. Dethloff and others (1996) used it to simulate the climate of the Arctic, and Van Meijgaard (1995) evaluated large-scale precipita-

tion events over Europe. In a study by Christensen and others (1996b), RACMO was evaluated for climate simulations over Europe. In the studies by Christensen and others (1996b) and Dethloff and others (1996), the model is referred to as HIRHAM. In this paper, the model with a resolution of 55 km × 55 km is evaluated for three sites in the Antarctic. Application of RACMO to the extreme meteorological conditions occurring in Antarctica is a severe test of the parameterisation of physical processes, which have been developed and evaluated mainly for data-rich areas. Therefore, the model has to be tested thoroughly before it can be used for the simulation of the mass balance of Antarctica. In this study, we will focus on the evaluation of mean temperature and humidity profiles during January 1993. A simulation with RACMO for this month is compared with in situ measurements done during the same period at three sites, i.e. the Amundsen–Scott South Polar station (SP), the Georg von Neumayer station (GvN) and the Swedish research station Svea located in Dronning Maud Land. The ability of the model to simulate the temperature and humidity profiles correctly is important in order to obtain correct moisture fluxes.

2. MEASUREMENTS

We used temperature and humidity profiles measured at three different locations to evaluate the model. Radiosonde measurements made at GvN and SP were used to evaluate model output at a gridpoint near the coast and at a gridpoint on the plateau of the ice cap, respectively (Fig. 1). GvN (70°39′ S, 8°15′ W) is located on the Ekström Ice Shelf in the Atlantic sector of Antarctica. The ice shelf has a flat, homogeneous surface sloping gently upwards toward the south. SP is located at a height of 2835 m a.s.l. on the flat plateau in the interior of the continent. January mean profiles of the atmosphere for 1993 were calculated from the daily balloon soundings. In austral summertime, the radiosondes reach a height of 25–35 km. The accuracy of the temperature, relative humidity and pressure measurements is $\pm 0.5°C$, $\pm 3\%$ and ± 0.5 hPa, respectively (König-Langlo and Herber, 1996).
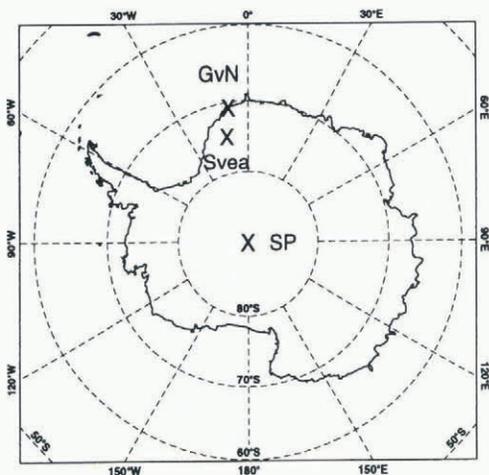

Fig. 1. Map of the location of Georg von Neumayer station (GvN; 70°39′ S, 8°15′ W), Amundsen–Scott South Polar station (SP; 90° S) and the Swedish station Svea (74°35′ S, 11°13′ W). Data measured at these sites are used to evaluate model output.

However, the high vertical velocity of the radiosonde causes additional temperature errors of the order of $5°C$ in the lowest 100 m of the atmosphere (Mahesh and others, 1997).

In the austral summer of 1992–93, detailed boundary-layer measurements were performed at Svea (74°35′ S 11°13′ W; Fig. 1) in Dronning Maud Land (Bintanja and others, 1993). Svea is located in a U-shaped valley, Scharffenbergbotnen, in the central part of the Heimefront Range at an elevation of 1250 m a.s.l. and at a distance of 290 km from the coast. A helium-filled cable balloon was launched every 3–6 h, provided the surface wind speed was less than 10 m s^{-1}. Pressure, temperature, humidity, wind speed and wind direction were measured in the lowest 800 m of the boundary layer (Van den Broeke and Bintanja, 1995). Because the area around Svea is characterised by rock outcrops and small valleys, wind speed and direction are determined by the local topography. Therefore it is useless to verify simulated wind speed and direction with these data, because model output is representative of an entire gridbox of 55 km × 55 km. Jonsson (1992) compared data from an automatic weather station (AWS50) located inside of the Scharffenbergbotnen valley to data from an AWS representative for the undisturbed area located 12 km northwest of AWS50. He found that during the period 18 January–18 February 1988, the temperature and specific humidity inside of the Scharffenbergbotnen valley were $2.4°C$ and 0.17 g kg^{-1} higher, respectively, than the temperature and humidity outside of this valley. The profiles at Svea were averaged over the period 14–19 January 1993 (P1), because fair weather made it possible to increase the number of balloon soundings to one sounding every 3 hours during this period.

3. ECMWF RE-ANALYSES

The re-analyses are constructed by reassimilating data for the period 1979–94 into a simulation with the ECMWF model at T106 resolution and 31 atmospheric vertical levels (Gibson and others, 1997). On the Antarctic continent, only a few radiosondes are launched and satellite data are not assimilated. Therefore the re-analyses depend largely on the model output. In situ measurements made at SP and at 12 stations near the coast, including GvN, are involved in the assimilation procedure. In this paper, temperature and humidity profiles available every 6 hours are compared with RACMO output and measured profiles.

4. THE MODEL

The model used in this study is a regional atmospheric climate model with a horizontal resolution of 55 km × 55 km (Christensen and others, 1996a). In the present configuration, the model has a grid with 122 × 130 points covering an area of 4.9×10^7 km^2, including the Antarctic continent and a large part of the Southern Ocean. The model grid is represented in Figure 2a. The topography of Drewry (1983) is used, and in Figure 2b the surface geopotential height of this database is shown along the cross-section, indicated by the vertical black line depicted in Figure 2a. The steep gradients in the coastal zone of the continent are resolved with roughly ten gridpoints. Twenty hybrid levels in the vertical (σ-coordinates near the surface transforming gradually into pressure coordinates) are employed, with the lowest levels centred at 8, 38, 139, 367 and 752 m.
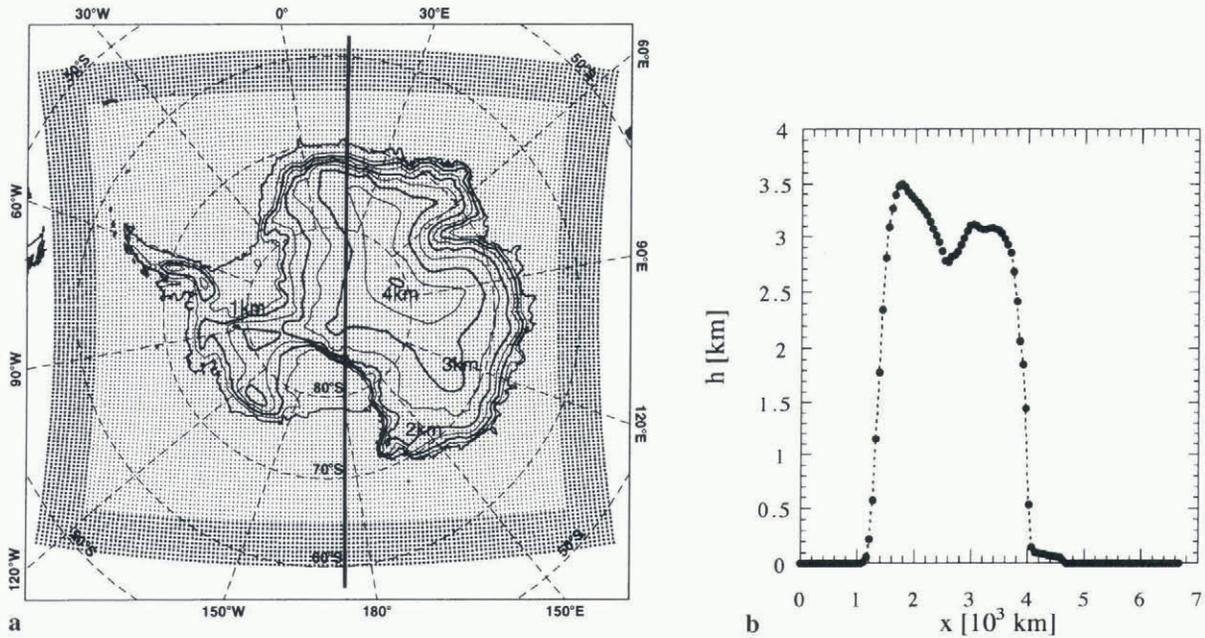
Fig. 2. (a) RACMO grid with a horizontal spacing of 55 km. In the relaxation zone (indicated by larger dots), the model prognostic variables are relaxed towards ECMWF re-analyses. The surface geopotential height (km) is indicated by the contour lines. (b) Model orography along the cross-section indicated by the black line in (a). Dots refer to model gridpoints.

The dynamical part of RACMO is taken from the high-resolution limited-area model (HIRLAM; Gustafsson, 1993), which was developed specifically for short-range weather forecasting. The parameterisations of the physical processes were taken from the general circulation or climate model (GCM) ECHAM4, which is used at the Max Planck Institute for Meteorology, Hamburg (Roeckner and others, 1996). A brief description of the various parameterisations is presented in Table 1. Before the model was applied to Antarctica, adjustments were made to the parameterisation of the albedo, the snow-temperature initialisation, the capacity and heat diffusivity of the snow and the surface roughness. These adjustments are described briefly in Table 1.

Sea-surface temperature and sea-ice mask were prescribed and updated every 6 hours by ECMWF re-analyses. The sea-ice mask is based on special sensor microwave/imager (SSM/I) satellite measurements (Nomura, 1995). A gridbox is either ice-free or uniformly covered with sea ice of a constant thickness. The sea-ice temperature is a prognostic variable, calculated from the surface energy budget and the heat flux from the ocean. In the lateral boundary zone of the model domain (larger dots in Figure 2a) the prognostic variables were relaxed towards ECMWF re-analyses using a technique proposed by Dickinson and others (1989). The ECMWF re-analyses, available every 6 hours, were linearly interpolated to obtain values at intermediate times at all time-steps. The model was initialised with the ECMWF re-analysis of 0000 UTC (Universal Time Co-ordinated) on 28 December 1992. Subsequently, an integration was performed covering the period 28 December 1992–31 January 1993 using a model time-step of 4 min. This run is referred to as the control run. From tendencies of the model prognostic variables, it appeared that the spin-up time in the model atmosphere is of the order of a few hours. However, it is possible that the spin-up time of the temperatures in the snow is a more serious problem. Therefore, temperature initialisation of the five snow layers is important. The sensitivity of the atmospheric profiles to initial snow temperatures will be discussed in the next section.

Table 1. Short description of the ECHAM4 parameterisations and the adjustments implemented before the model was applied for Antarctica

|	
Surface fluxes and vertical diffusion	Turbulent fluxes at the surface are calculated from Monin–Obukhov similarity theory. Approximate analytical expressions derived by Louis (1979) for the transfer coefficients are used. A higher-order closure based on the formulation by Brinkop and Roeckner (1995) is used to compute turbulent transfer within and above the boundary layer in which eddy diffusivity is expressed in terms of turbulent kinetic energy. The effective roughness length is introduced to account for the effects of sub-grid terrain effects and sub-grid orography. The effective roughness length is taken from the ECMWF model.
Land surface processes	The heat diffusion equation is solved for five soil layers with zero heat flux at a depth of 10 m. The original ECHAM4 code is adjusted by implementing heat diffusivity and capacity of snow.
Gravity wave drag	Drag associated with orographic waves is simulated using directional-dependent sub-grid-scale orographical variances obtained from the high-resolution Drewry dataset (Miller and others, 1989).
Cumulus convection	Bulk mass concept for shallow, mid-level and deep convection (Tiedtke, 1989).
Stratiform clouds	Budget equations for water vapour and cloud water (prognostic variable) (Sundqvist, 1978)
Radiation	Broadband flux emissivity method with six longwave bands and two-stream formulation with two shortwave intervals (Fouquart and Bonnel, 1980; Morcrette and others, 1986). In the ECHAM4 code, the albedo is parameterised as a function of temperature. This, however, does not correspond to albedo measurements. Therefore a constant albedo of 0.8 is prescribed in the adjusted code.
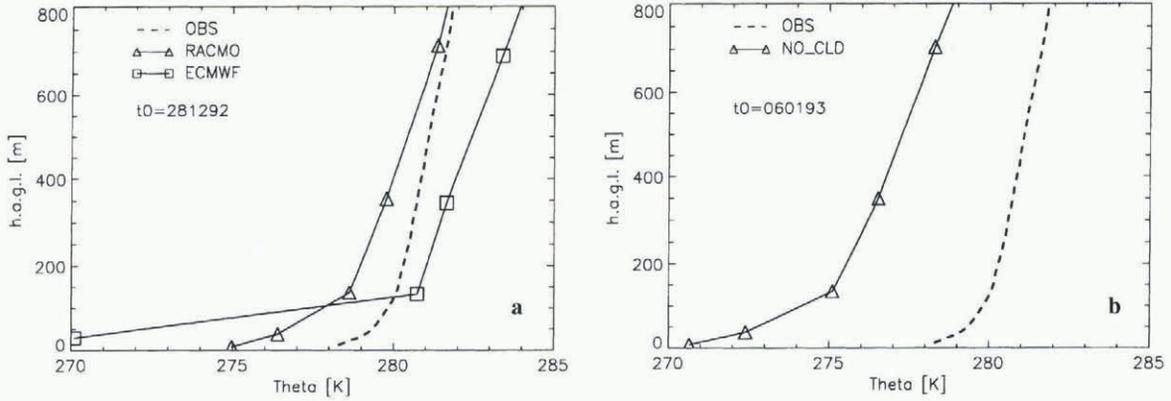
Fig. 3. Mean potential temperature profiles at Svea averaged over the period 14–19 January 1993 as a function of height above ground level (h.a.g.l.). The observed profiles (OBS) are plotted together with the control run, ECMWF re-analyses (a) and the sensitivity run NO_CLD (b). In the NO_CLD simulation, the radiation calculations are performed for clear sky conditions at all gridpoints for the entire period of simulation. The control run is initialised on 28 December 1992 (t0) and the NO_CLD run is initialised on 6 January 1993.

5. RESULTS

5.1. Temperature profiles

Model output and measurements at Svea are analyzed only for the period 14–19 January 1993 (P1). Mean measured and simulated potential temperature profiles are displayed in Figure 3 together with ECMWF re-analyses. From Figure 3a it can be seen that the simulated temperatures are somewhat lower than the measured temperatures. However, the model is representative for an area of 55 km × 55 km, whereas the measurements are performed only at one site, namely, in the Scharffenbergbotnen valley. The horizontal variability discussed in section 2 largely explains the difference between simulated and measured absolute temperatures. The simulated lapse rate $(\partial T/\partial z)$ at Svea is somewhat larger than the measured lapse rate. However, the difference between the simulated and measured lapse rate is much smaller than the difference between ECMWF re-analyses and observations. As a result of an unrealistically large vertical temperature gradient in the lowest two model layers of the atmosphere, turbulent transport is largely suppressed in the re-analysis.

ECMWF re-analyses at the gridpoints close to Svea depend largely on the first guess of the ECMWF model. After all, Svea is located a considerable distance from any station whose observations are assimilated in the re-analysis. Therefore, the difference between RACMO output and ECMWF re-analyses in boundary-layer temperature profiles is likely to be related to differences between RACMO and the ECMWF model, and not to the assimilation of data into the re-analysis system. It is likely that the differences in the model output are caused by the use of different vertical diffusion schemes. The parameterisations used in RACMO originate from the global ECHAM4 model. In both ECHAM and ECMWF the vertical diffusion in the boundary layer is based on the eddy diffusivity concept (K-theory). This formulation is known to underestimate heat exchange in stable conditions. In the ECMWF model, the extension into the free atmosphere is based on continuation of the similarity theory. This is not the case in the ECHAM4 scheme. Instead, the latter uses a 1.5-order closure, based on a formulation by Brinkop and Roeckner (1995), in which the eddy diffusivity is expressed in terms of

turbulent kinetic energy. Apparently, heat exchange in stable conditions is somewhat enhanced by this formulation, resulting in better agreement between simulation and measurements. Nevertheless, the profiles suggest that the heat exchange generated with the ECHAM4 scheme is still insufficient. Another difference between the ECMWF model and the ECHAM4 model is the value of the absorption coefficients for the water-vapour continuum in the radiation code. However, a simulation with RACMO employing the absorption coefficients of the ECMWF model clearly showed that the difference in the radiation code cannot be the sole explanation for the differences found between the two models in the simulated temperature profiles.

Although period P1 at Svea was characterised by a mean cloud cover of less than 0.5 octas, a mean cloud cover of 2.4 octas at a height of 5 km was simulated by the model. A sensitivity simulation (NO_CLD) was performed in which radiation calculations for all gridpoints were performed for clear sky conditions. This simulation does not give a proper representation of clouds in the atmosphere either, because clouds were present at locations other than Svea during P1. The NO_CLD run is useful for studying the sensitivity of the temperature profiles to cloud cover. Because only period P1 was analyzed, the model was initialised on 6 January 1993. In the run NO_CLD, a decrease in longwave flux at the surface was partly compensated by an increase in incoming shortwave radiation. Therefore, the net radiation at the surface is only 2.1 W m^{-2} smaller in the NO_CLD run. Clouds have a warming effect on the boundary layer at Svea (Fig. 3b) due to an increase of incoming longwave radiation at the top of the boundary layer. From Figure 3a it seemed that the absolute temperature was represented well by RACMO at Svea. This, however, could be an artefact of the presence of spurious clouds in the model.

During P1, balloon soundings at Svea were made every 3 hours. Therefore, these data are used to evaluate the simulated daily cycle of the boundary-layer temperature. In Figure 4a, the observed daily cycle averaged over P1 is shown. At 1245 UTC the highest solar elevation is reached at Svea, and a maximum in temperature is observed at 1500 UTC. The shortwave radiation is positive during the entire period, but we will refer to the period of small incoming solar radiation as "the night". From 1900 to 0600 UTC when incoming solar radiation is small, the net heat flux is
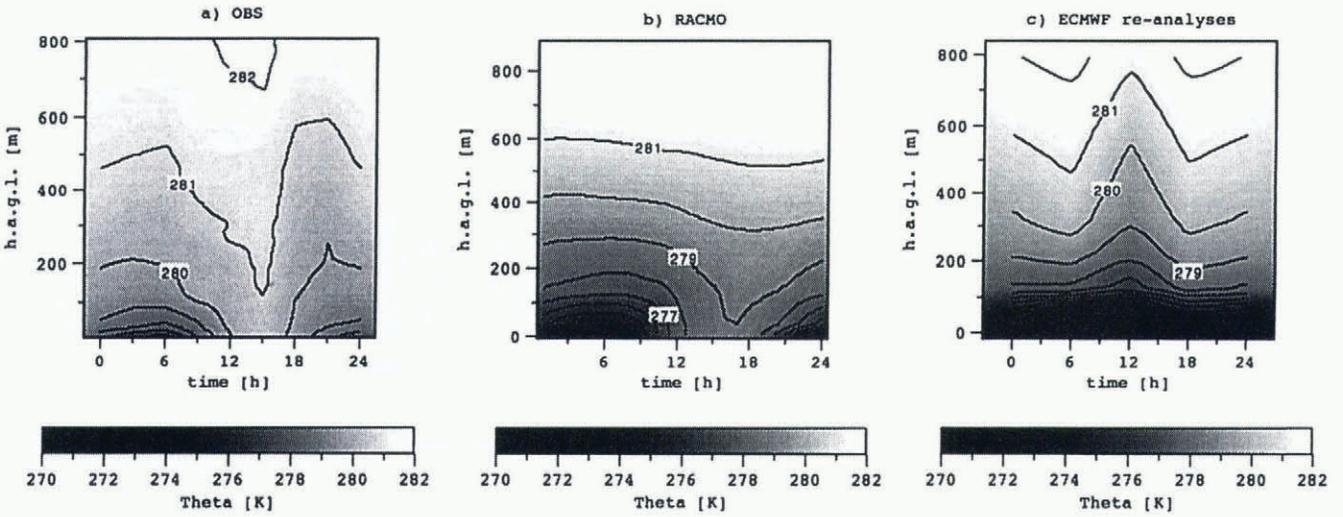
Fig. 4. Daily cycle of the potential temperature in the boundary layer at Svea averaged over P1.

directed away from the surface, and a statically stable boundary layer develops. The daily cycle in boundary-layer temperature is fairly well represented by the RACMO model (Fig. 4b). However, the simulated lapse rate during "the night" is too large. The correspondence in lapse rate between model and measurements is much better during "daytime". The simulated amplitude of the temperature signal above 200 m is too small, indicating that "daytime" turbulent transport is underestimated in the model. The maximum in atmospheric temperature is simulated somewhat too late. In the re-analyses the lowest atmospheric

layer is decoupled from the rest of the atmosphere (Fig. 4c). A very high temperature gradient between the lowest and the second lowest layer is present, even during "daytime". The surface temperature signal cannot propagate to higher levels, because heat exchange between the lowest two levels is largely suppressed in this situation.

At GvN and SP, the radiosonde data and the model output were analyzed for the entire month of January 1993. Averaged over this period, the atmosphere is stably stratified at all sites. Contrary to the findings at Svea, good agreement is found between the ECMWF re-analysis and the
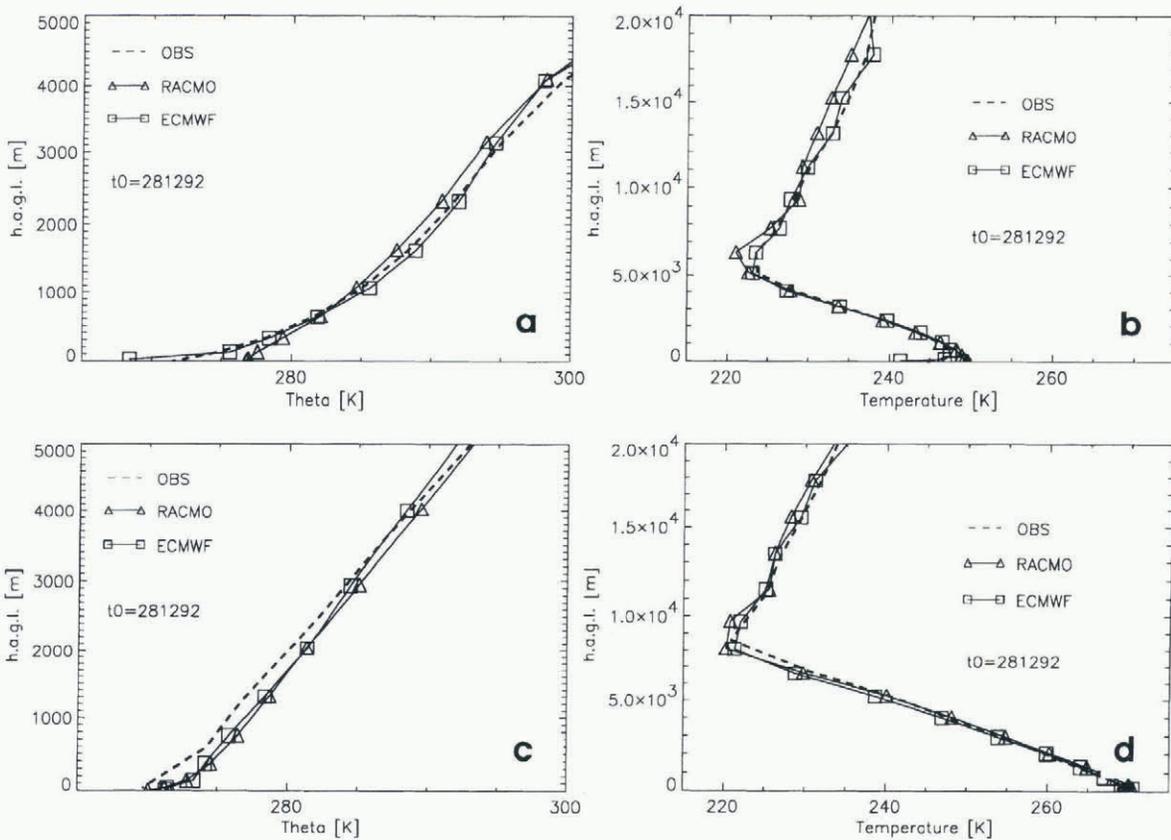

Fig. 5. January mean profiles at SP (a, b) and GvN (c, d) stations. Left panels show the potential temperature profiles in the atmosphere to a height of 5 km; right panels show the temperature profile in the atmosphere to a height of 20 km. At GvN, the RACMO output and ECMWF re-analyses of 1200 UTC were used to calculate the average profiles, because this time corresponds most closely to the time of the balloon launches.
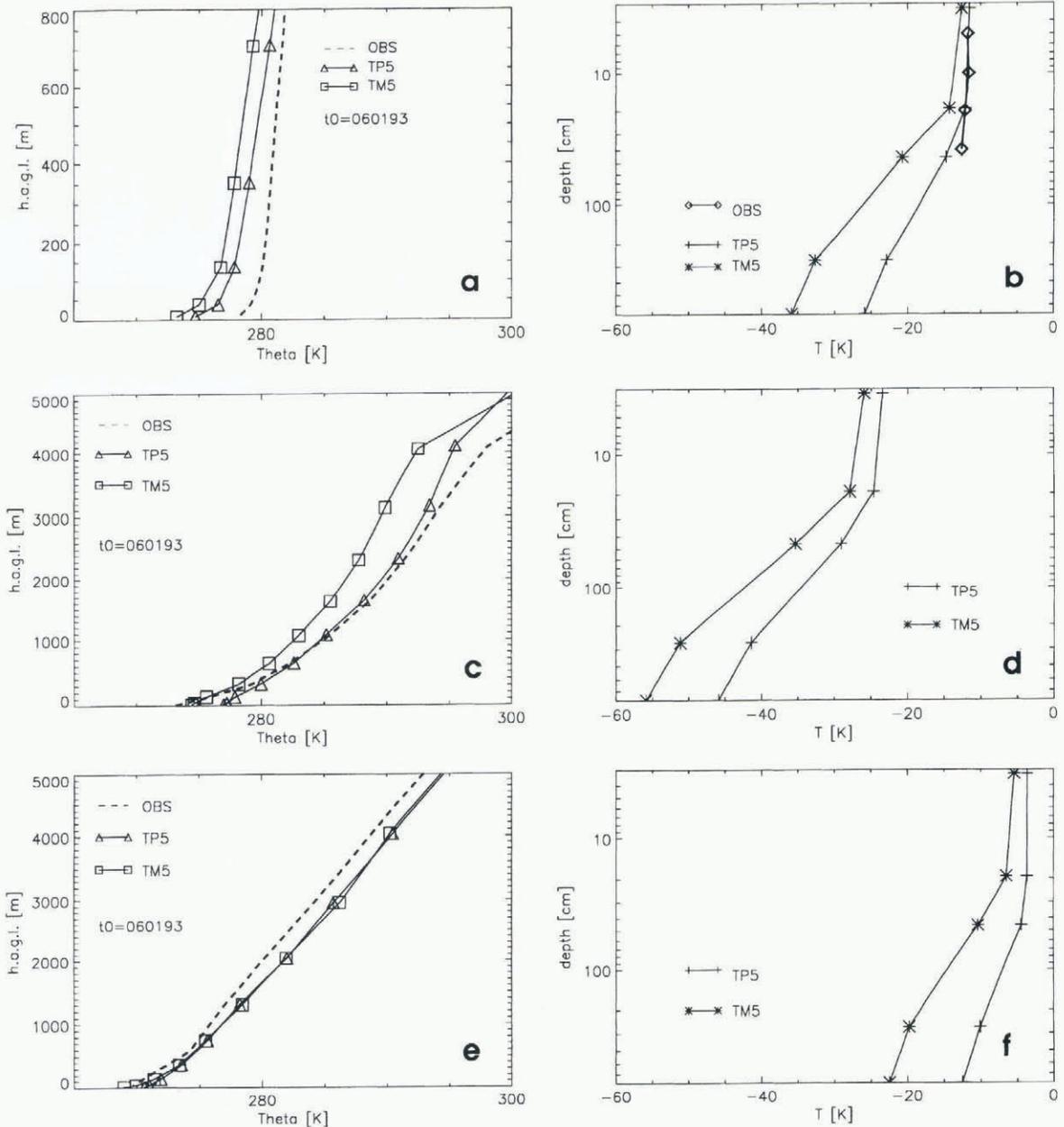
Fig. 6. Mean profiles over the period 14–19 January 1993 (P1) at Svea (a, b), SP (c, d) and GvN (e, f) for the sensitivity runs TP5 and TM5. In TP5 and TM5 the snow temperature of all land points is initialised 5 °C higher and 5 °C lower, respectively, than in the standard initialisation. The left column displays the simulated and observed mean potential temperature profiles in the atmosphere. When comparing these figures directly to those in Figures 3 and 5 it should be borne in mind that a different date of initialisation (t0) is chosen, and that the profiles for GvN and SP in Figures 3 and 5 are averaged over January and not over P1. In the right column, the mean temperature profiles over P1 in the snow are displayed for the two sensitivity runs. In addition, measurements from the surface to a depth of 80 cm are shown in (b). The simulated cloud cover can be different in the two sensitivity runs; this can have a large impact on the temperature profiles.

measurements at SP and GvN (Fig. 5). Radiosonde measurements from these two stations are used in the data assimilation procedure. RACMO generated realistic temperature profiles at SP and GvN with biases smaller than 5°C. At both SP and GvN the simulated lapse rate is slightly too small in the troposphere. At GvN, the simulated lapse rate in the boundary layer was larger than the measurements indicate, but no conclusion can be drawn from this difference, because the accuracy of radiosonde close to the surface is not very high (Mahesh and others, 1997). From Figure 5b and d it can be seen that at both SP and GvN the simulated temperatures in the stratosphere and at the tropopause were too low. A cold bias in polar higher troposphere and lower stratosphere up to 15 K in summer is also present in most

present-day GCMs (Boer and others, 1992; Roeckner and others, 1996).

5.2. Snow-temperature initialisation

The time-scale for spin-up of temperature in the deeper snow layers is much longer than the length of the simulation. For this reason, the model is expected to be sensitive to the temperature initialisation in the snow. The temperature initialisation is taken from a climatology, and the model snow-temperature profile is most likely not identical to the real snow-temperature profiles in Antarctica at the time of initialisation. Accordingly, two sensitivity studies, TP5 and TM5, were performed, in which the temperature
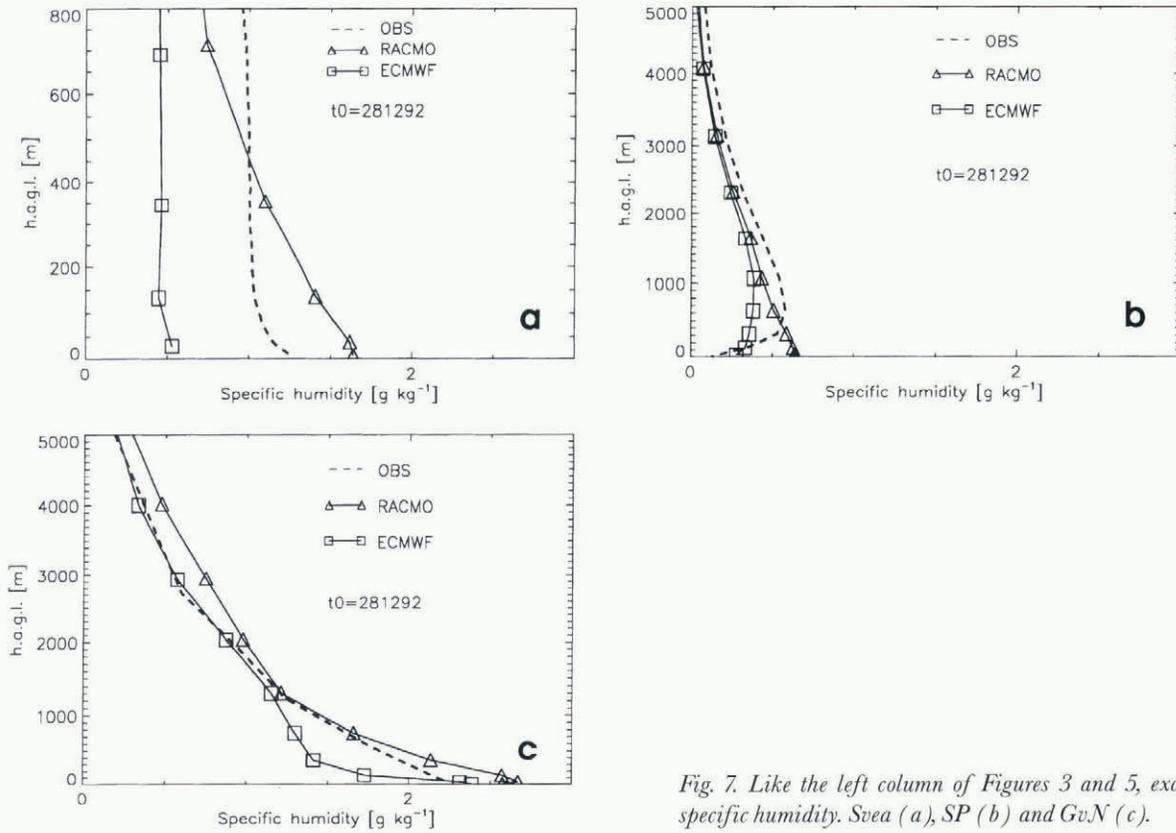
Fig. 7. Like the left column of Figures 3 and 5, except for specific humidity. Svea (a), SP (b) and GvN (c).

of all snow layers was initialised 5°C higher and 5°C lower, respectively, than in the reference initialisation.

From Figure 6a, c and e it can be seen that snow-temperature initialisation has a minor effect on the simulated lapse rate in the atmosphere. Therefore, it is concluded that the differences in simulated and measured atmospheric lapse rate as shown in Figures 3 and 5 cannot be explained by improper snow-temperature initialisation. However, the absolute value of the atmospheric temperature was affected by the initialisation. The difference between TP5 and TM5 is largest at SP, which is located farthest from the coast. Therefore, all gridpoints in an extensive surrounding area of SP were initialised 10°C colder in TM5 than in TP5. This caused a difference in tropospheric temperature of roughly 3.7°C. The initial energetic difference between the two runs corresponds to an absolute temperature difference of 11.2°C in an entire atmospheric column with a surface pressure of 700 hPa. At GvN, initialisation has the smallest effect on the atmospheric temperature, because the gridbox is surrounded by sea and sea-ice points. At all sites, the difference in surface temperatures (T_s) between TP5 and TM5 is smaller than 2.5°C, because T_s depends largely on the meteorological conditions. Consequently, the vertical temperature gradient in the snow and the accompanying heat flux into the deeper layers is larger in TM5 than in TP5.

5.3. Humidity profiles

To simulate realistic humidity profiles, the model has to simulate correct temperature profiles. Errors in simulated vertical temperature gradients affect the exchange coefficients for moisture. Above, we already concluded that the lapse rate of the ECMWF re-analyses is too high. Therefore, turbulent transport of moisture was suppressed, resulting in too dry tropospheric profiles (Fig. 7). Although the error in the humidity measurements and the horizontal variability

(section 2) is large, it cannot explain the difference of 0.5 g kg^{-1} found between the ECMWF re-analyses and the measurements. Again, the difference between the ECMWF re-analyses and the observations at Svea are most pronounced. The atmosphere simulated by RACMO contains more moisture than the ECMWF re-analyzed atmosphere, and therefore the simulated amount of water vapour in the atmosphere is in better agreement with the observations. At all sites, however, the simulated humidity near the surface is too high. Humidity decreases too fast with height, supporting the previous statement that turbulent transport to higher levels is still insufficient in the model. At SP, the observed specific-humidity profiles exhibit a maximum at 500 m. RACMO is unable to simulate this maximum. The model is most successful at simulating the specific humidity at GvN.

6. SUMMARY

The ability of RACMO to simulate the mean temperature and humidity profiles at three different sites at Antarctica has been discussed in this paper. The boundary layer up to 800 m measured at Svea was analyzed for the period 14–19 January 1993. The difference between simulated and observed temperature is smaller than the horizontal variability. However, the cloud cover at the gridpoints corresponding to Svea is overestimated, which has a warming effect on the boundary layer. The simulated lapse rate and the lapse rate in the re-analyses are too high, but the simulation corresponds much better to the observations than do the ECMWF re-analyses. In the re-analyses, a decoupling of the lowest model layer from the higher layers in the atmosphere occurs, so turbulent transport is largely suppressed. The daily cycle is represented fairly well by the model, although the amplitude of the temperature signal above 200 m is somewhat too small. At GvN and SP, January mean

profiles were measured up to a height of 25–35 km. The simulated lapse rate in the troposphere is too low. Temperatures in the stratosphere and at the tropopause are too low, but the absolute temperature difference remains within 5°C. Sensitivity studies reveal that the differences in the lapse rate between the model and the measurements cannot be explained by improper snow initialisation.

Although the measurements of humidity in cold regions are subject to considerable uncertainties, they indicate that the relative humidity in the lowest atmospheric layers is higher than the measured relative humidity. This supports the statement that turbulent transport of moisture to higher levels is insufficient in the model. The agreement between model and measurements is largest at GvN.

It is concluded that the model is capable of simulating the vertical temperature profiles reasonably well, but considerable differences between simulated and measured vertical humidity profiles are present. In the future, we intend to perform longer integrations to obtain a model climatology of the mass balance. Although the comparison with observations indicates that the model has some deficiencies, especially with respect to the turbulent transport of moisture in the boundary layer, fairly good agreement between observations and simulations gives us confidence that the model can be used for mass-balance simulations.

REFERENCES

Bintanja, R., M. R. van den Broeke and M. P. Portanger. 1993. *A meteorological and glaciological experiment on a blue ice area in the Heimefront Range, Queen Maud Land, Antarctica.* Utrecht, Utrecht University, Institute for Marine and Atmospheric Research. (SVEA 1992/93 Field Report.)

Boer, G. J. *and 13 others.* 1992. Some results from an intercomparison of the climate simulated by 14 atmospheric general circulation models. *J. Geophys. Res.*, 97 (D12), 12,771–12,786.

Brinkop, S. and E. Roeckner. 1995. Sensitivity of a general circulation model to parameterisations of cloud–turbulence interactions in the atmospheric boundary layer. *Tellus*, 47A (2), 197–220.

Bromwich, D. H. 1988. Snowfall in high southern latitudes. *Rev. Geophys.*, 26 (1), 149–168.

Bromwich, D. H., B. Chen and R.-Y. Tzeng. 1995. Arctic and Antarctic precipitation simulations produced by the NCAR community climate models. *Ann. Glaciol.*, 21, 117–122.

Budd, W. F., P. A. Reid and L. J. Minty. 1995. Antarctic moisture flux and net accumulation from global atmospheric analyses. *Ann. Glaciol.*, 21, 149–156.

Christensen, J. H., O. B. Christensen, P. Lopez, E. van Meijgaard and M. Botzet. 1996a. *The HIRHAM 4 regional atmospheric climate model.* Copenhagen, Danish Meteorological Institute. (DMI Scientific Report 96-4.)

Christensen, J. H. *and 6 others.* 1996b. *Validation of present-day regional climate simulations over Europe: LAM simulations with observed boundary conditions.* Copenhagen, Danish Meteorological Institute. (DMI Scientific Report 96-10.)

Connolley, W. M. and H. Cattle. 1994. The Antarctic climate of the UKMO unified model. *Antarct. Sci.*, 6 (1), 115–122.

Connolley, W. M. and J. C. King. 1996. A modeling and observational study of East Antarctic surface mass balance. *J. Geophys. Res.*, 101 (D1), 1335–1344.

Dethloff, K., A. Rinke, R. Lehmann, J. H. Christensen, M. Botzet and B. Machenhauer. 1996. A regional climate model of the Arctic atmosphere. *J. Geophys. Res.*, 101 (D18), 23,401–23,422.

Dickinson, R. E., R. M. Errico, F. Giorgi and G. T. Bates. 1989. A regional climate model for the western United States. *Climatic Change*, 15 (3), 383–422.

Drewry, D. J., *ed.*. 1983. *Antarctica: glaciological and geophysical folio.* Cambridge, University of Cambridge, Scott Polar Research Institute.

Engels, R. and G. Heinemann. 1996. Three-dimensional structures of summertime Antarctic mesoscale cyclones. Part 2. Numerical simulations with a limited area model. *The Global Atmosphere and Ocean System*, 4, 181–208.

Fouquart, Y. and B. Bonnel. 1980. Computations of solar heating of the Earth's atmosphere: a new parameterization. *Beitr. Phys. Atmos.*, 53 (1), 35–62.

Genthon, C. 1994. Antarctic climate modeling with general circulation models of the atmosphere. *J. Geophys. Res.*, 99 (D6), 12,953–12,961.

Gibson, R., P. Kållberg, S. Uppala, A. Hernandez, A. Nomura and E. Serrano. 1997. *ERA description.* Reading, European Centre for Medium-Range Weather Forecasts. (ECMWF Re-Analysis Project Report Series 1.)

Giovinetto, M. B. and C. R. Bentley. 1985. Surface balance in ice drainage systems of Antarctica. *Antarct. J. U.S.*, 20 (4), 6–13.

Gustafsson, N. 1993. *HIRLAM 2 final report.* Norrköping, Sveriges Meteorologiska och Hydrologiska Institut (SMHI). (HIRLAM Technical Report 9.)

Hines, K. M., D. H. Bromwich and T. R. Parish. 1995. A mesoscale modeling study of the atmospheric circulation of high southern latitudes. *Mon. Weather Rev.*, 123 (4), 1146–1165.

Jonsson, S. 1992. Local climate and mass balance of a blue-ice area in western Dronning Maud Land, Antarctica. *Z. Gletscherkd. Glazialgeol.*, 26 (1), 1990, 11–29.

König-Langlo, G. and A. Herber. 1996. Meteorological data of the Neumayer Station (Antarctica) for 1992, 1993, and 1994. *Ber. Polarforsch.* 187.

Louis, J. F. 1979. A parametric model of vertical eddy fluxes in the atmosphere. *Boundary-Layer Meteorol.*, 17 (2), 187–202.

Mahesh, A., V. P. Walden and S. G. Warren. 1997. Radiosonde temperature measurements in strong inversions: correction for thermal lag based on an experiment at the South Pole. *J. Atmos. Oceanic Technol.*, 14, 45–53.

Marsiat, I. 1996. Ice-sheets' surface mass-balance evaluation in the UGAMP GCM: the climate of Antarctica. *Ann. Glaciol.*, 23, 167–173.

Miller, M. J., T. N. Palmer and R. Swinbank. 1989. Parameterization and influence of sub-grid scale orography in general circulation and numerical weather prediction models. *Meteorol. Atmos. Phys.*, 40 (1–3), 84–109.

Morcrette, J. -J., L. Smith and Y. Fouquart. 1986. Pressure and temperature dependence of the absorption in longwave radiation calculations. *Beitr. Phys. Atmos.*, 59 (4), 455–469.

Nomura, A. 1995. *Global sea ice concentration data set for use with the ECMWF re-analysis system.* Reading, European Centre for Medium-Range Weather Forecasts. Re-Analysis Project (ERA). (Technical Report 76.)

Ohmura, A., M. Wild and L. Bengtsson. 1996. A possible change in mass balance of Greenland and Antarctic ice sheets in the coming century. *J. Climate*, 9 (9), 2124–2135.

Roeckner, E. *and 9 others.* 1996. *The atmospheric general circulation model ECHAM-4: model description and simulation of present day climate.* Hamburg, Max-Planck-Institut für Meteorologie. (Report 218.)

Sundqvist, H. 1978. A parameterization scheme for non-convective condensation including prediction of cloud water content. *Q. J. R. Meteorol. Soc.*, 104 (441), 677–690.

Tiedtke, M. 1989. A comprehensive mass flux scheme for cumulus parameterization in large-scale models. *Mon. Weather Rev.*, 117 (8), 1779–1800.

Tzeng, R.-Y., D. H. Bromwich, T. R. Parish and B. Chen. 1994. NCAR CCM2 simulation of the modern Antarctic climate. *J. Geophys. Res.*, 99 (D11), 23,131–23,148.

Van den Broeke, M. R. and R. Bintanja. 1995. Summertime atmospheric circulation in the vicinity of a blue ice area in east Queen Maud Land, Antarctica. *Boundary-Layer Meteorol.*, 72 (45), 411–438.

Van Meijgaard, E. 1995. Precipitation forecasts from atmospheric models during recent flooding events of the Meuse. *Phys. Chem. Earth*, 20, 497–502.

Walsh, K. and J. L. McGregor. 1996. Simulations of the Antarctic climate using a limited area model. *J. Geophys. Res.*, 101 (D14), 19,093–19,108.